

# ANALYSIS OF MESH EFFECTS ON TURBULENT FLOW STATISTICS

ALI PAKZAD

ALP145@PITT.EDU

DEPARTMENT OF MATHEMATICS  
UNIVERSITY OF PITTSBURGH

**ABSTRACT.** Turbulence models, such as the Smagorinsky model herein, are used to represent the energy lost from resolved to under-resolved scales due to the energy cascade (i.e. non-linearity). Analytic estimates of the energy dissipation rates of a few turbulence models have recently appeared, but none (yet) study energy dissipation restricted to resolved scales, i.e. after spacial discretization with  $h >$  micro scale. We do so herein for the Smagorinsky model. Upper bounds are derived on the *computed* time-averaged energy dissipation rate,  $\langle \varepsilon(u^h) \rangle$ , for an under-resolved mesh  $h$  for turbulent shear flow. For coarse mesh size  $\mathcal{O}(\mathcal{R}e^{-1}) < h < L$ , it is proven,

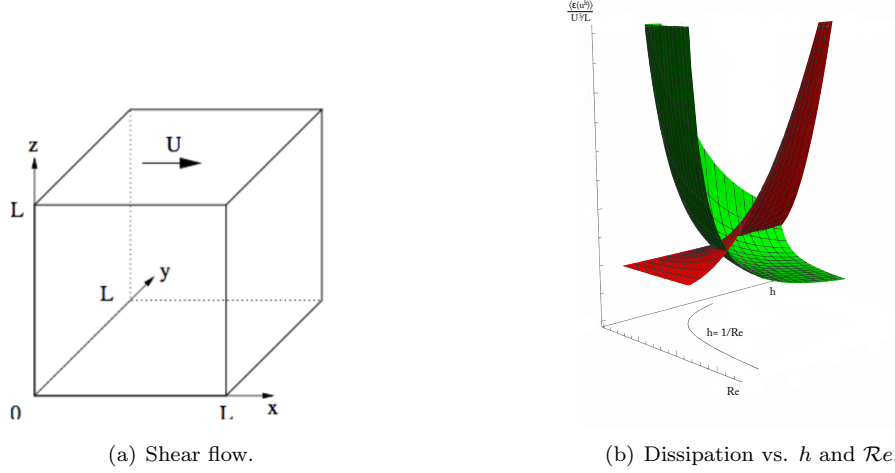
$$\langle \varepsilon(u^h) \rangle \leq \left[ \left( \frac{C_s \delta}{h} \right)^2 + \frac{L^5}{(C_s \delta)^4 h} + \frac{L^{\frac{5}{2}}}{(C_s \delta)^4} h^{\frac{3}{2}} \right] \frac{U^3}{L},$$

where  $U$  and  $L$  are global velocity and length scale and  $C_s$  and  $\delta$  are model parameters. This upper bound is independent of the viscosity at high Reynolds number, is in accord with the scaling theory of turbulent. This estimate suggests over-dissipation for any of  $C_s > 0$  and  $\delta > 0$ , consistent with numerical evidence on the effects of model viscosity (without wall damping function). Moreover, the analysis indicates that the turbulent boundary layer is a more important length scale for shear flow than the Kolmogorov microscale.

## 1. INTRODUCTION

Because of the limitations of computers, we are forced to struggle with the meaning of under-resolved flow simulations. Turbulence models are introduced to account for sub-mesh scale effects, when solving fluid flow problems numerically. One key in getting a good approximation for a turbulent model is to correctly calibrate the energy dissipation  $\varepsilon(u)$  in the model on an under-resolved mesh. Energy dissipation rates of various turbulent models have been analyzed assuming infinite resolution (i.e. for the continuous model e.g. [9], [23], [24], [28], [35] and [46]). The question explored herein is: What is the time-averaged energy dissipation rate  $\langle \varepsilon(u^h) \rangle$ , when  $u^h$  is an approximation of  $u$  on a given mesh  $h$  (fixed computational cost) for the Smagorinsky model?

Numerical simulations of turbulent flows include only the motion of eddies above some length scale  $\delta$  (which depends on attainable resolution). The state of motion in turbulence is too complex to allow for a detailed description of the fluid velocity. Benchmarks are required to validate simulations' accuracy. Two natural benchmarks for numerical simulations are the kinetic energy in the eddies of size  $> \mathcal{O}(\delta)$  and the energy dissipation rates of eddies in size  $> \mathcal{O}(\delta)$  (e.g. [32] and [19]). Motivated from here, we focus on the calculation of the time-averaged energy dissipation rates of motions larger than  $\delta$ . In the large-eddy simulation (LES), predicting how flow statistics (e.g. time-averaged) depend on the grid size  $h$  and the filter size  $\delta$  is listed as one of ten important questions by Pope [36].



Consider the Smagorinsky model (1.1) subject to a boundary-induced shear (1.2) in the flow domain  $\Omega = (0, L)^3$ ,

$$(1.1) \quad \begin{aligned} u_t + u \cdot \nabla u - \nu \Delta u + \nabla p - \nabla \cdot ((C_s \delta)^2 |\nabla u| \nabla u) &= 0, \\ \nabla \cdot u &= 0 \quad \text{and} \quad u(x, 0) = u_0 \quad \text{in } \Omega. \end{aligned}$$

In (1.1)  $u$  is the velocity field,  $p$  is the pressure,  $\nu$  is the kinematic viscosity,  $\delta$  is the turbulence-resolution length scale (associated with the mesh size  $h$ ) and  $C_s \simeq 0.1$  is the standard model parameter (see Lilly [26] for more details). We consider shear flow, containing a turbulent boundary layer, in a domain that is simplified to permit more precise analysis.  $L$ -periodic boundary conditions in  $x$  and  $y$  directions are imposed.  $z = 0$  is a fixed wall and the wall  $z = L$  moves with velocity  $U$  (Figure 1(a)),

$$(1.2) \quad \begin{aligned} L - \text{periodic boundary condition in } x \text{ and } y \text{ direction,} \\ u(x, y, 0, t) = (0, 0, 0)^\top \quad \text{and} \quad u(x, y, L, t) = (U, 0, 0)^\top. \end{aligned}$$

To disregard the effects of the time discretization on dissipation, we consider (1.1) continuous in time and discretized in space (see (2.6)) by a standard finite element method since the effects of the spacial discretization, and not the time discretization, on dissipation is the subject of study here. In Theorem 3.1, we first estimate  $\langle \varepsilon(u^h) \rangle$  for fine enough mesh that no model to be necessary ( $h < \mathcal{O}(\mathcal{R}e^{-1}) L$ ). Since models are used for meshes coarser than a DNS, we next investigate (1.1) on an arbitrary coarse mesh. Theorem 3.3 presents the analysis of  $\langle \varepsilon(u^h) \rangle$  on an under-resolved mesh. The results in Theorems 3.1 and 3.3 can be summarized as,

$$(1.3) \quad \frac{\langle \varepsilon(u^h) \rangle}{U^3 / L} \simeq \begin{cases} 1 + \left(\frac{C_s \delta}{L}\right)^2 \mathcal{R}e^2 & \text{for } h < \mathcal{O}(\mathcal{R}e^{-1}) L \\ \frac{1}{\mathcal{R}e} \frac{L}{h} + \left(\frac{C_s \delta}{h}\right)^2 + \frac{L^5}{(C_s \delta)^4 h} + \frac{L^{\frac{5}{2}}}{(C_s \delta)^4} h^{\frac{3}{2}} & \text{for } h \geq \mathcal{O}(\mathcal{R}e^{-1}) L \end{cases}.$$

Considering  $\delta = h$  in (1.3), which is the common choice in LES [36], we speculate that  $\frac{\langle \varepsilon(u^h) \rangle}{U^3 / L}$  varies with  $\mathcal{R}e$  and  $h$  as depicted qualitatively in figure 1(b).

*Remark 1.1.* Shear flow has two natural microscales. The Kolmogorov microscale is  $\eta \simeq \mathcal{R}e^{-\frac{3}{4}} L$ , and describes the size of the smallest persistent motion away from walls. The second, turbulent boundary layer, length is  $\mathcal{R}e^{-1} L$ . Our analysis here, and (1.3), indicates this latter scale is the more important one for shear flow.

$\langle \varepsilon(u^h) \rangle$  in (1.3) scales as  $\frac{U^3}{L}$  as predicted by Richardson and Kolmogorov. For the fully-resolved case, this estimate is consistent as  $\mathcal{R}e \rightarrow \infty$  and  $\delta = h \simeq \mathcal{O}(\mathcal{R}e^{-1})$  with the rate proven for the Navier-Stokes equations in [9]. On the other hand, the weak  $\mathcal{R}e$  dependence in the under-resolved case (that vanishes as  $\mathcal{R}e \rightarrow \infty$ ) is consistent with the Figure 1, adopted from [11]. This figure shows how dissipation coefficient varies with Reynolds number for circular cylinder based on experimental data quoted in [44]. Tritton [44] observed that dissipation coefficient behaves as  $\mathcal{R}e^{-1}$  for small  $\mathcal{R}e$ , and at high  $\mathcal{R}e$  stays approximately constant. Theorem 3.3 is also consistent with the recent results in [30] derived through structure function theories of turbulence.

Corollaries 3.6 and 3.8 show that the estimate (1.3) suggests over-dissipation of the model for any chose of  $C_s > 0$  and  $\delta > 0$ . In other words, constant  $C_s$  causes excessive damping of large-scale fluctuation, which agrees the computational experience (p.247 of Sagaut [40]). There are several model refinements to reduce this over dissipation such as the damping function [35].

In Sections 2, we collect necessary mathematical tools. In Section 3, the major results are proven. We end this report with numerical illustrations and conclusions in Sections 4 and 5.

**1.1. Motivation and Related Works.** In turbulence, dissipation predominantly occurs at small scales. Once a mesh (of size  $h$ ) is selected, an eddy viscosity term  $\nabla \cdot ((C_s \delta)^2 |\nabla u| \nabla u)$  in (1.1) with  $\delta = \mathcal{O}(h)$  is added to the Navier-Stokes equations (NSE),  $C_s = 0$  in (1.1), to model this extra dissipation which can not be captured by the NSE viscous term on an under-resolved mesh.

Turbulence is about prediction of velocities' averages rather than the point-wise velocity. One commonly used average in turbulent flow modeling is time-averaging. Time averages seem to be predictable even when dynamic flow behavior over bounded time intervals is irregular [11]. Time averaging is defined in terms of the limit superior ( $\limsup$ ) of a function as,

$$\langle \psi(\cdot) \rangle = \limsup_{T \rightarrow \infty} \frac{1}{T} \int_0^T \psi(t) dt.$$

The classical **scaling theory of turbulence** is based on the concept of the energy cascade. Energy is input into the largest scales of the flow, then the kinetic energy cascade from large to small scale of motions. When it reaches a scale small enough for viscous dissipation to be effective, it dissipates mostly into heat (Richardson 1922, [38]). Since viscous dissipation is negligible through this cascade, the energy dissipation

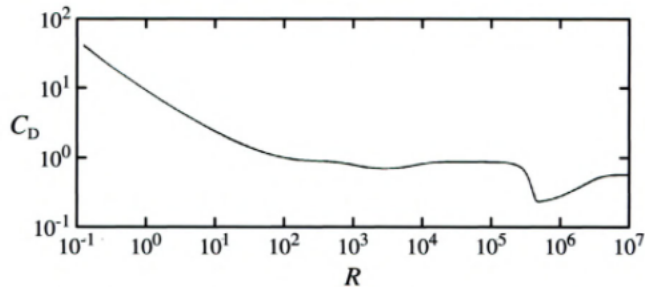


FIGURE 1. Variation of dissipation coefficient with Reynolds number for circular cylinder.

rate is related then to the power input to the largest scales at the first step in the cascade. These largest eddies have energy  $\frac{1}{2}U^2$  and time scale  $\tau = \frac{L}{U}$ , this implies the equilibrium dissipation law for time-averaged energy dissipation rate  $\langle \varepsilon \rangle$  (Kolmogorov 1941),

$$\langle \varepsilon \rangle = \mathcal{O}\left(\frac{U^2}{\tau}\right) \simeq C_\varepsilon \frac{U^3}{L},$$

with  $C_\varepsilon = \text{constant}$ . Saffman [39], addressing the estimate of energy dissipation rates,  $\langle \varepsilon \rangle \simeq \frac{U^3}{L}$ , and wrote that,

*This result is fundamental to an understanding of turbulence and yet still lacks theoretical support.*

Information about  $C_\varepsilon$  carries interesting information about the structure of the turbulent flow. Therefore mathematically rigorous upper bounds on  $C_\varepsilon$  are of high relevance. There are many analytical, numerical and experimental evidence to support the equilibrium dissipation law as some of them are mentioned below.

Taylor [43] considered  $C_\varepsilon$  to be constant for geometrically similar boundaries. His work leaded to the question "If  $C_\varepsilon$  depends on geometry, boundary and inlet conditions". Since then, a multitude of laboratory experiments [42] and numerical simulations [5] concerned with isotropic homogeneous turbulence seem to confirm that  $C_\varepsilon$  is independent of Reynolds number in the limit of high Reynolds number, but are not conclusive as to whether  $C_\varepsilon$  is universal at such high Reynolds number values. In fact, the high Reynolds number values of  $C_\varepsilon$  seem to differ from flow to flow. The first results in 3D obtained for turbulent shear flow between parallel plates by Howard [18] and Busse [7] under assumptions that the flow is statistically stationary. There is an asymptotic non-zero upper bound,  $C_\varepsilon \simeq 0.01$  as  $\mathcal{Re} \rightarrow \infty$ , first derived by Busse [7] (Joining dashed line in Figure 2). The lower bound on  $C_\varepsilon$  is already given for laminar flow by Doering and Constantin,  $\frac{1}{\mathcal{Re}} \leq C_\varepsilon$  (solid slanted straight line in Figure 2). Rigorous asymptotic  $\mathcal{Re} \rightarrow \infty$  dissipation rate bounds of the form  $\langle \varepsilon \rangle \leq C_\varepsilon \frac{U^3}{L}$ , with  $C_\varepsilon \simeq 0.088$  (topmost horizontal solid line in Figure 2), were derived for a number of boundary-driven flows during the 1990s (Doering and Constantin [9]). The residual dissipation bound like this appeared for a shear layer turbulent Taylor-Couette flow- where  $L$  was the layer thickness and  $U$  was the overall velocity drop across the layer. The upper bound has been confirmed with higher precision in [34] as  $C_\varepsilon \simeq 0.01087$  (Heavy dots in Figure 2). The corresponding experimental data measured

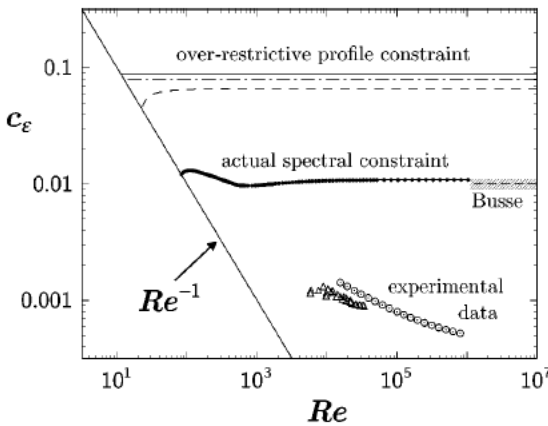


FIGURE 2.  $C_\varepsilon$  versus  $\mathcal{Re}$ , adopted from [33].

by Reichardt [37] for the plane Couette flow (Triangles in Figure 2) and by Lathrop, Fineberg, and Swinney [22] for the small-gap Taylor-Couette system (Circles in Figure 2).

### 1.2. Why the Eddy Viscosity model and not the Navier Stokes?

A shear flow is one where the boundary condition is tangential. The flow problem with the boundary condition like (1.2) becomes very close to the flow between rotating cylinders. Flow between rotating cylinders is one of the classic problems in experimental fluid dynamics (e.g. [11]).

Consider the Navier Stokes equations,  $C_s = 0$  in (1.1), with the boundary condition (1.2). The difficulty in the analysis of energy dissipation of the shear flow appears due to the effect of the non-homogeneous boundary condition on the flow. The classical approach is required to construct careful and non-intuitive choice of background flow  $\Phi$  known as the Hopf extension [17].

**Definition 1.1.** Let  $\Phi(x, y, z) := (\phi(z), 0, 0)^\top$ , where,

$$(1.4) \quad \phi(z) = \begin{cases} 0 & \text{if } z \in [0, L-h] \\ \frac{U}{h}(z - L + h) & \text{if } z \in [L-h, L] \end{cases}.$$

The strategy is to subtract off the inhomogeneous boundary conditions (1.2). Consider  $v = u - \Phi$ , then  $v$  satisfies homogeneous boundary conditions. Substituting  $u = v + \Phi$  in the NSE yields,

$$(1.5) \quad \begin{aligned} v_t + v \cdot \nabla v - \nu \Delta v + \nabla p + \phi(z) \frac{\partial v}{\partial x} + v_3 \phi'(z) (1, 0, 0) &= \nu \phi''(z) (1, 0, 0), \\ \nabla \cdot v &= 0. \end{aligned}$$

The key idea in making progress in the mathematical understanding of the energy dissipation rate is the energy inequality. Taking inner product (1.5) with  $v = (v_1, v_2, v_3)$  and integrating over  $\Omega$  gives,

$$(1.6) \quad \frac{1}{2} \frac{\partial}{\partial t} \|v\|^2 + \nu \|\nabla v\|^2 + \int_{\Omega} \left( \phi(z) \frac{\partial v}{\partial x} \cdot v + v_1 v_3 \phi'(z) \right) dx = \int_{\Omega} \nu \phi''(z) v_1 dx.$$

However the NSE are rewritten to make the viscous term easy to handle, the nonlinear term changes and must again be wrestled with. To calculate energy dissipation, the non-linear terms should be controlled by the diffusion term. Since both terms are quadratic in  $u$ , considering current tools in analysis, this control is doable only by assuming  $h$  in Definition 1.1 being small. Doering and Constantin [9] used the NSE to find an upper bound on the time -averaged energy dissipation rate for shear driven turbulence, assuming  $h \simeq \mathcal{R}e^{-1}$ . Similar estimations have been proven by Marchiano [28], Wang [46] and Kerswell [21] in more generality. For the semi-discrete NSE, John, Layton and Manica [20] could show that assuming infinite resolution near the boundaries, computed time averaged energy dissipation rate  $\langle \varepsilon(u^h) \rangle$  for the shear flow scales as predicted for the continuous flow by the Kolmogorov theory,

$$\langle \varepsilon(u^h) \rangle \simeq \frac{U^3}{L}.$$

Now the question arises: How to find  $\langle \varepsilon(u^h) \rangle$  for shear driven turbulence without any restriction on the mesh size? With current analysis tools, the effort seems to be hopeless. Therefore the p-laplacian term,

$$(1.7) \quad \nabla \cdot (|\nabla u|^{p-2} \nabla u),$$

was added to the NSE. This modification will lead to the a  $p^{\text{th}}$  – degree term on the left side of the energy inequality. Then applying appropriate Youngs inequality on the non-linear term, we will absorb it on the  $p^{\text{th}}$  – degree term without any restriction on  $h$ . Herein, we focus on  $p = 3$  (the Smagorinsky model (1.1)), but the analysis for  $p > 3$  remains as an interesting problem.

## 2. MATHEMATICAL PRELIMINARIES, NOTATIONS AND DEFINITIONS

We use the standard notations  $L^p(\Omega)$ ,  $W^{k,p}(\Omega)$ ,  $H^k(\Omega) = W^{k,2}(\Omega)$  for the Lebesgue and Sobolev spaces respectively. The inner product in the space  $L^2(\Omega)$  will be denoted by  $(\cdot, \cdot)$  and its norm by  $\|\cdot\|$  for scalar, vector and tensor quantities. Norms in Sobolev spaces  $H^k(\Omega)$ ,  $k > 0$ , are denoted by  $\|\cdot\|_{H^k}$  and the usual  $L^p$  norm is denoted by  $\|\cdot\|_p$ . The symbols  $C$  and  $C_i$  for  $i = 1, 2, 3$  stand for generic positive constant independent of the  $\nu$ ,  $L$  and  $U$ . In addition,  $\nabla u$  is the gradient tensor  $(\nabla u)_{ij} = \frac{\partial u_i}{\partial x_j}$  for  $i, j = 1, 2, 3$ .

The Reynolds number is  $\mathcal{R}e = \frac{UL}{\nu}$ . The time-averaged energy dissipation rate for model (1.1) includes dissipation due to the viscous forces and the turbulent diffusion. It is given by,

$$(2.1) \quad \langle \varepsilon(u) \rangle = \limsup_{T \rightarrow \infty} \frac{1}{T} \int_0^T \left( \frac{1}{|\Omega|} \int_{\Omega} \nu |\nabla u|^2 + (c_s \delta)^2 |\nabla u|^3 dx \right) dt.$$

**Definition 2.1.** The velocity at a given time  $t$  is sought in the space

$$\mathbb{X}(\Omega) := \{u \in H^1(\Omega) : u(x, y, 0) = (0, 0, 0)^\top, u(x, y, L) = (U, 0, 0)^\top, u \text{ is } L\text{-periodic in } x \text{ and } y \text{ direction}\}.$$

The test function space is

$$\mathbb{X}_0(\Omega) := \{u \in H^1(\Omega) : u(x, y, 0) = (0, 0, 0)^\top, u(x, y, L) = (0, 0, 0)^\top, u \text{ is } L\text{-periodic in } x \text{ and } y \text{ direction}\}.$$

The pressure at time  $t$  is sought in

$$Q(\Omega) := L^2_0(\Omega) = \{q \in L^2(\Omega) : \int_{\Omega} q dx = 0\}.$$

And the space of divergence-free functions is denoted by

$$V(\Omega) := \{u \in \mathbb{X}(\Omega) : (\nabla \cdot u, q) = 0 \quad \forall q \in Q\}.$$

**Lemma 2.1.**  $\Phi$  in Definition 1.1 satisfies,

- a)  $\|\Phi\|_{\infty} \leq U$ ,
- b)  $\|\nabla \Phi\|_{\infty} \leq \frac{U}{h}$ ,
- c)  $\|\Phi\|^2 \leq \frac{U^2 L^2 h}{3}$ ,
- d)  $\|\nabla \Phi\|^2 \leq \frac{U^2 L^2}{h}$ ,
- e)  $\|\nabla \Phi\|_3^3 \leq \frac{U^3 L^2}{h^2}$ ,
- f)  $\|\nabla \Phi\|_{\frac{3}{2}}^3 = \frac{U^3 L^4}{h^2}$ .

*Proof.* They all are the immediate consequences of the Definition 1.1.  $\square$

*Remark 2.2.*  $\Phi$  extends the boundary conditions (1.2) to the interior of  $\Omega$ . Moreover, it is a divergence-free function.  $h \in (0, L)$  stands for the spacial mesh size.

Using standard scaling argument in the next lemma shows how the constant  $C_{\ell}$  in the Sobolev inequality  $\|u\|_6 \leq C_{\ell} \|\nabla u\|_3$  depends on the geometry in  $\mathbb{R}^3$ .

**Lemma 2.3.** Consider the Sobolev inequality  $\|u\|_6 \leq C_{\ell} \|\nabla u\|_3$ , then  $C_{\ell}$  is the order of  $L^{\frac{1}{2}}$  when domain is  $\Omega = [0, L]^3$ , i.e.

$$\|u\|_6 \leq C L^{\frac{1}{2}} \|\nabla u\|_3.$$

*Proof.* Let  $\Omega = [0, L]^3$ ,  $\hat{\Omega} = [0, 1]^3$  and for simplicity  $x = (x_1, x_2, x_3)$  and  $\hat{x} = (\hat{x}_1, \hat{x}_2, \hat{x}_3)$ . Consider the change of variable  $\eta : \hat{\Omega} \rightarrow \Omega$  by  $\eta(\hat{x}) = L \hat{x} = x$ . If  $u(L\hat{x}) = \hat{u}(\hat{x})$ , using the chain rule gives,

$$\frac{d}{d\hat{x}_i} (\hat{u}(\hat{x})) = \frac{d}{d\hat{x}_i} (u(L\hat{x})) = L \frac{du}{dx_i}(L\hat{x}),$$

for  $i = 1, 2, 3$  and since  $L\hat{x} = x$  we have,

$$(2.2) \quad \frac{1}{L} \frac{d\hat{u}}{d\hat{x}_i} = \frac{du}{dx_i}.$$

Using (2.2) and the change of variable formula, one can show,

$$\left\| \frac{\partial u_i}{\partial x_j} \right\|_3^3 = \int_{\Omega} \left| \frac{\partial u_i}{\partial x_j} \right|^3 dx = \int_{\hat{\Omega}} \frac{1}{L^3} \left| \frac{\partial \hat{u}_i}{\partial \hat{x}_j} \right|^3 L^3 d\hat{x} = \left\| \frac{\partial \hat{u}_i}{\partial \hat{x}_j} \right\|_3^3,$$

therefore,

$$(2.3) \quad \|\nabla u\|_3^3 = \sum_{i,j=1}^3 \left\| \frac{\partial u_i}{\partial x_j} \right\|_3^3 = \sum_{i,j=1}^3 \left\| \frac{\partial \hat{u}_i}{\partial \hat{x}_j} \right\|_3^3 = \|\hat{\nabla} \hat{u}\|_3^3.$$

Again by applying the change of variable formula, we have,

$$\|u\|_{L^6(\Omega)} = \left( \int_{\Omega} |u|^6 dx \right)^{\frac{1}{6}} = \left( \int_{\hat{\Omega}} L^3 |\hat{u}|^6 d\hat{x} \right)^{\frac{1}{6}} = L^{\frac{1}{2}} \|\hat{u}\|_{L^6(\hat{\Omega})},$$

using the Sobolev inequality and also inequality (2.3) on the above equality leads to,

$$(2.4) \quad \|\hat{u}\|_{L^6(\hat{\Omega})} = L^{-\frac{1}{2}} \|u\|_{L^6(\Omega)} \leq L^{-\frac{1}{2}} C_{\ell} \|\nabla u\|_3 = L^{-\frac{1}{2}} C_{\ell} \|\hat{\nabla} \hat{u}\|_3,$$

therefore as claimed  $C_{\ell} = \mathcal{O}(L^{\frac{1}{2}})$ .  $\square$

We will need the well-known dependence of the Poincaré -Friedrichs inequality constant on the domain. A straightforward argument in the thin domain  $\mathcal{O}_h$  implies Lemma 2.4.

**Lemma 2.4.** *Let  $\mathcal{O}_h = \{(x, y, z) \in \Omega : L - h \leq z \leq L\}$  be the region close to the upper boundary. Then we have*

$$(2.5) \quad \|u - \Phi\|_{L^2(\mathcal{O}_h)} \leq h \|\nabla(u - \Phi)\|_{L^2(\mathcal{O}_h)}.$$

*Proof.* The proof is standard.  $\square$

**2.1. Variational Formulation and Discretization.** The variational formulation is obtained by taking the scalar product  $v \in \mathbb{X}_0$  and  $q \in L_0^2$  with (1.1) and integrating over the space  $\Omega$ .

$$(2.6) \quad \begin{aligned} (u_t, v) + \nu(\nabla u, \nabla v) + (u \cdot \nabla u, v) - (p, \nabla \cdot v) + ((C_s \delta)^2 |\nabla u| \nabla u, \nabla v) &= 0 \quad \forall v \in \mathbb{X}_0, \\ (\nabla \cdot u, q) &= 0 \quad \forall q \in L_0^2, \\ (u(x, 0) - u_0(x), v) &= 0 \quad \forall v \in \mathbb{X}_0. \end{aligned}$$

To discretize the SM, consider two finite-dimensional spaces  $\mathbb{X}^h \subset \mathbb{X}$  and  $\mathbb{Q}^h \subset \mathbb{Q}$  satisfy the following discrete inf-sup condition where  $\beta^h > 0$  uniformly in  $h$  as  $h \rightarrow 0$ ,

$$(2.7) \quad \inf_{q^h \in \mathbb{Q}^h} \sup_{v^h \in X^h} \frac{(q^h, \nabla \cdot v^h)}{\|\nabla v^h\| \|q^h\|} \geq \beta^h > 0.$$

The inf-sup condition (2.7) plays a significant role in studies of the finite-element approximation of the Navier-Stokes equations. It is usually taken as a criterion of whether or not the families of finite-element spaces yield stable approximations. In the other word, it ensures given the unique velocity, there is a corresponding pressure. It is also critical to bounding the fluid pressure and showing the pressure is stable.

Consider a subspace  $V^h \subset \mathbb{X}^h$  by,

$$V^h := \{v^h \in X^h : (q^h, \nabla \cdot v^h) = 0, \forall q^h \in \mathbb{Q}^h\}.$$

Note that most often  $V^h \not\subset V$  and  $\nabla \cdot u^h \neq 0$  for any  $u^h \in V^h$ . Thus we need an extension of the trilinear from  $(u \cdot \nabla v, w)$  as follows.

**Definition 2.2. (Trilinear form)** Define the trilinear form  $b$  on  $\mathbb{X} \times \mathbb{X} \times \mathbb{X}$  as,

$$b(u, v, w) := \frac{1}{2}(u \cdot \nabla v, w) - \frac{1}{2}(u \cdot \nabla w, v).$$

**Lemma 2.5.** *The nonlinear term  $b(\cdot, \cdot, \cdot)$  is continuous on  $\mathbb{X} \times \mathbb{X} \times \mathbb{X}$  (and thus on  $V \times V \times V$  as well). Moreover, we have the following skew-symmetry properties for  $b(\cdot, \cdot, \cdot)$ ,*

$$b(u, v, w) = (u \cdot \nabla v, w) \quad \forall u \in V \text{ and } v, w \in \mathbb{X},$$

Moreover,

$$b(u, v, v) = 0 \quad \forall u, v \in \mathbb{X}.$$

*Proof.* The proof is standard, see p.114 of Girault and Raviart [14].  $\square$

The semi-discrete/continuous-in-time finite element approximation continues by selecting finite element spaces  $\mathbb{X}_0^h \subset \mathbb{X}_0$ . The approximate velocity and pressure of the Smagorinsky problem (1.1) are  $u^h : [0, T] \rightarrow \mathbb{X}^h$  and  $p^h : (0, T] \rightarrow \mathbb{Q}^h$  such that,

$$(2.8) \quad \begin{aligned} (u_t^h, v^h) + \nu(\nabla u^h, \nabla v^h) + b(u^h, u^h, v^h) - (p^h, \nabla \cdot v^h) + (C_s \delta)^2 |\nabla u^h| \nabla u^h, \nabla v^h) &= 0 \quad \forall v^h \in \mathbb{X}_0^h, \\ (\nabla \cdot u^h, q^h) &= 0 \quad \forall q^h \in \mathbb{Q}^h, \\ (u^h(x, 0) - u_0(x), v^h) &= 0 \quad \forall v^h \in \mathbb{X}_0^h. \end{aligned}$$

### 3. THEOREMS AND PROOFS

In the following theorems, we present upper bounds on the computed time-averaged energy dissipation rate for the Smagorinsky model (1.1) subject to the shear flow boundary condition (1.2). Theorem 3.1 consider the case when the mesh size is fine enough  $h < \mathcal{O}(\mathcal{R}e^{-1})L$ . The restriction on the mesh size arises from the mathematical analysis of constructible background flow in finite element space.

On the other hand, Theorem 3.3 investigates  $\langle \varepsilon(u^h) \rangle$  for any mesh size  $0 < h < L$ . We then take a minimum of two bounds to find the optimal upper bound in (1.3) with respect to current analysis.

**Theorem 3.1. (fully-resolved mesh)** Suppose  $u_0 \in L^2(\Omega)$  and mesh size  $h < (\frac{1}{5}\mathcal{R}e^{-1})L$ . Then  $\langle \varepsilon(u^h) \rangle$  satisfies,

$$\langle \varepsilon(u^h) \rangle \leq C \left[ 1 + \left( \frac{c_s \delta}{L} \right)^2 \mathcal{R}e^2 \right] \frac{U^3}{L}.$$

*Proof.* Let  $h = \gamma L$  in Definition 1.1 for  $0 < \gamma < L$ . Take  $v^h = u^h - \Phi \in \mathbb{X}_0^h$  in (2.8). Since  $b(\cdot, \cdot, \cdot)$  is skew-symmetric (Lemma 2.5) and  $\nabla \cdot \Phi = 0$ , we have,

$$(u_t^h, u^h - \Phi) + \nu(\nabla u^h, \nabla u^h - \nabla \Phi) + b(u^h, u^h, u^h - \Phi) + ((C_s \delta)^2 |\nabla u^h| \nabla u^h, \nabla u^h - \nabla \Phi) = 0,$$

and integrate in time to get,

$$(3.1) \quad \begin{aligned} \frac{1}{2} \|u^h(T)\|^2 - \frac{1}{2} \|u^h(0)\|^2 + \nu \int_0^T \|\nabla u^h\|^2 dt + \int_0^T \left( \int_{\Omega} (C_s \delta)^2 |\nabla u^h|^3 dx \right) dt &= (u^h(T), \Phi) - (u^h(0), \Phi) \\ &+ \int_0^T b(u^h, u^h, \Phi) dt + \nu \int_0^T (\nabla u^h, \nabla \Phi) dt + (C_s \delta)^2 \int_0^T (|\nabla u^h| \nabla u^h, \nabla \Phi) dt. \end{aligned}$$

Using the Cauchy-Schwarz Young inequality and Lemma 2.1 for  $h = \gamma L$  to bound the right-hand side of the above energy equality.

$$(3.2) \quad (u^h(T), \Phi) \leq \frac{1}{2} \|u^h(T)\|^2 + \frac{1}{2} \|\Phi\|^2 = \frac{1}{2} \|u^h(T)\|^2 + \frac{U^2 \gamma L^3}{6}.$$

$$(3.3) \quad (u^h(0), \Phi) \leq \|u^h(0)\| \|\Phi\| = \sqrt{\frac{\gamma}{3}} U L^{\frac{3}{2}} \|u^h(0)\|.$$

$$(3.4) \quad \nu \int_0^T (\nabla u^h, \nabla \Phi) dt \leq \frac{\nu}{2} \int_0^T \|\nabla u^h\|^2 + \|\nabla \Phi\|^2 dt = \frac{\nu}{2} \int_0^T \|\nabla u^h\|^2 dt + \frac{\nu}{2} \frac{U^2 L}{\gamma} T.$$

Next, the nonlinear term  $b(\cdot, \cdot, \cdot)$  in (3.1) can be rewritten as,

$$(3.5) \quad \begin{aligned} b(u^h, u^h, \Phi) &= b(u^h - \Phi, u^h - \Phi, \Phi) + b(\Phi, u^h - \Phi, \Phi) \\ &= \frac{1}{2} b(u^h - \Phi, u^h - \Phi, \Phi) - \frac{1}{2} b(u^h - \Phi, \Phi, u^h - \Phi) \\ &\quad + \frac{1}{2} b(\Phi, u^h - \Phi, \Phi) - \frac{1}{2} b(\Phi, \Phi, u^h - \Phi). \end{aligned}$$

Each term in (3.5) is estimated separately as follows using Lemma 2.4 and the Cauchy-Schwarz Young inequality. For the first term in (3.5) we have,

$$(3.6) \quad \begin{aligned} b(u^h - \Phi, u^h - \Phi, \Phi) &\leq \|\Phi\|_{L^\infty} \|u^h - \Phi\|_{L^2} \|\nabla(u^h - \Phi)\|_{L^2} \leq \gamma L U \|\nabla(u^h - \Phi)\|_{L^2}^2 \\ &\leq \gamma L U \|\nabla u^h - \nabla \Phi\|_{L^2}^2 \leq U L \gamma (\|\nabla u^h\| + \|\nabla \Phi\|)^2 \leq U L \gamma (2\|\nabla u^h\|^2 + 2\|\nabla \Phi\|^2) \\ &\leq U L \gamma (2\|\nabla u^h\|^2 + 2\frac{U^2 L}{\gamma}) = 2 U L \gamma \|\nabla u^h\|^2 + 2 U^3 L^2. \end{aligned}$$

For the second term we have,

$$(3.7) \quad \begin{aligned} b(u^h - \Phi, \Phi, u^h - \Phi) &\leq \|\nabla \Phi\|_{L^\infty} \|u^h - \Phi\|^2 \leq \frac{U}{\gamma L} \gamma^2 L^2 \|\nabla(u^h - \Phi)\|^2 \\ &\leq \gamma^2 L^2 \frac{U}{\gamma L} (2\|\nabla u^h\|^2 + 2\frac{U^2 L}{\gamma}) = 2 \gamma L U \|\nabla u^h\|^2 + 2 U^3 L^2. \end{aligned}$$

The third one is estimated as,

$$(3.8) \quad \begin{aligned} b(\Phi, u^h - \Phi, \Phi) &\leq \|\Phi\|_{L^\infty} \|\nabla(u^h - \Phi)\|_{L^2} \|\Phi\|_{L^2} \leq U \sqrt{\frac{U^2 \gamma L^3}{3}} (\|\nabla u^h\| + \|\nabla \Phi\|) \\ &\leq U \sqrt{\frac{U^2 \gamma L^3}{3}} (\|\nabla u^h\| + \sqrt{\frac{U^2 L}{\gamma}}) \leq \frac{U^2 \gamma^{\frac{1}{2}} L^{\frac{3}{2}}}{\sqrt{3}} \|\nabla u^h\| + \frac{U^3 L^2}{\sqrt{3}} \\ &= \left[ \frac{U^{\frac{3}{2}} L}{\sqrt{3}} \right] [(U \gamma L)^{\frac{1}{2}} \|\nabla u^h\|] + \frac{U^3 L^2}{\sqrt{3}} \leq \left( \frac{U^3 L^2}{6} \right) + \frac{1}{2} U L \gamma \|\nabla u^h\|^2 + \frac{U^3 L^2}{\sqrt{3}} \\ &= \frac{1}{2} U L \gamma \|\nabla u^h\|^2 + \left( \frac{\sqrt{3}}{3} + \frac{1}{6} \right) U^3 L^2. \end{aligned}$$

And finally the last one satisfies,

$$\begin{aligned}
b(\Phi, \Phi, u^h - \Phi) &\leq \|\Phi\|_{L^\infty} \|\nabla \Phi\|_{L^2} \|u^h - \Phi\|_{L^2} \leq U \sqrt{\frac{U^2 L}{\gamma}} \gamma L \|\nabla(u^h - \Phi)\|_{L^2} \\
(3.9) \quad &\leq U^2 \gamma^{\frac{1}{2}} L^{\frac{3}{2}} (\|\nabla u^h\| + \|\nabla \Phi\|) \leq U^2 \gamma^{\frac{1}{2}} L^{\frac{3}{2}} (\|\nabla u^h\| + (\frac{U^2 L}{\gamma})^{\frac{1}{2}}) \\
&= U^2 \gamma^{\frac{1}{2}} L^{\frac{3}{2}} \|\nabla u^h\| + U^3 L^2 = [U^{\frac{3}{2}} L] [(U L \gamma)^{\frac{1}{2}} \|\nabla u^h\|] + U^3 L^2 \\
&\leq \frac{1}{2} (U^3 L^2) + \frac{1}{2} U L \gamma \|\nabla u^h\|^2 + U^3 L^2 = \frac{1}{2} U L \gamma \|\nabla u^h\|^2 + \frac{3}{2} U^3 L^2.
\end{aligned}$$

Use (3.6), (3.7), (3.8) and (3.9) in (3.5) gives the final estimation for the non-linear term as below.

$$(3.10) \quad |b(u^h, u^h, \Phi)| \leq \frac{5}{2} U L \gamma \|\nabla u^h\|^2 + \frac{19}{6} U^3 L^2.$$

Finally, Using Hölder's inequality and Young inequality for  $p = \frac{3}{2}$  and  $q = 3$  and lemma 2.3 on the last term gives,

$$\begin{aligned}
(|\nabla u^h| \nabla u^h, \nabla \Phi)| &\leq \int_{\Omega} |\nabla u^h|^2 \cdot \nabla \Phi \, dx \\
(3.11) \quad &\leq \left( \int_{\Omega} |\nabla u^h|^3 \right)^{\frac{2}{3}} \left( \int_{\Omega} |\nabla \Phi|^3 \right)^{\frac{1}{3}} \\
&\leq \frac{2}{3} \left( \int_{\Omega} |\nabla u^h|^3 \right) + \frac{1}{3} \left( \int_{\Omega} |\nabla \Phi|^3 \right) \leq \frac{2}{3} \left( \int_{\Omega} |\nabla u^h|^3 \right) + \frac{1}{3} \frac{U^3}{\gamma^2}.
\end{aligned}$$

Inserting (3.2), (3.3), (3.4), (3.10) and (3.11) in (3.1) implies,

$$\begin{aligned}
(3.12) \quad &\left( \frac{\nu}{2} - \frac{5}{2} \gamma L U \right) \int_0^T \|\nabla u^h\|^2 \, dt + \frac{1}{3} \int_0^T \left( \int_{\Omega} (C_s \delta)^2 |\nabla u^h|^3 \, dx \right) dt \leq \frac{1}{2} \|u^h(0)\|^2 + \frac{1}{6} U^2 \gamma L^3 \\
&+ \sqrt{\frac{\gamma}{3}} U L^{\frac{3}{2}} \|u^h(0)\| + \frac{19}{6} U^3 L^2 T + \frac{\nu}{2\gamma} L U^2 T + \frac{1}{3} (C_s \delta)^2 \frac{U^3 T}{\gamma^2}.
\end{aligned}$$

Dividing (3.12) by  $T$  and  $|\Omega| = L^3$  and taking limsup as  $T \rightarrow \infty$  lead to,

$$\min\left\{\frac{1}{2} - \frac{5}{2} \frac{\gamma L U}{\nu}, \frac{1}{3}\right\} \langle \varepsilon(u^h) \rangle \leq \frac{19}{6} \frac{U^3}{L} + \frac{\nu}{2\gamma} \frac{U^2}{L^2} + \frac{1}{3} (C_s \delta)^2 \frac{U^3}{\gamma^2 L^3}.$$

Let  $\gamma < \frac{1}{5} \mathcal{R}e^{-1}$ , then  $\min\left\{\frac{1}{2} - \frac{5}{2} \frac{\gamma L U}{\nu}, \frac{1}{3}\right\} > 0$  and the above estimates becomes,

$$\langle \varepsilon(u^h) \rangle \leq C \left[ 1 + \left( \frac{C_s \delta}{L} \right)^2 \mathcal{R}e^2 \right] \frac{U^3}{L},$$

which proves the theorem.  $\square$

*Remark 3.2.* The kinetic energy,  $\frac{1}{2} \|u^h\|^2$ , is not required in the proof to be uniformly bounded in time since it was canceled out from both sides after inserting (3.2) in (3.1).

The estimate in Theorem 3.1 goes to  $\frac{U^3}{L}$  for fixed  $\mathcal{R}e$  as  $C_s \delta \rightarrow 0$ , which is consistent with the rate proven for NSE by Doering and Constantin [9]. But it over dissipates for fixed  $\delta$  as  $\mathcal{R}e \rightarrow \infty$  as derived for the continuous case by Layton [24]. To fix this issue, one can suggests a super fine filter size  $\delta \simeq \frac{1}{\mathcal{R}e}$  which is not practical due to the computation cost. From here, we are motivated to study the following under-resolved case.

**Theorem 3.3. (under-resolved mesh)** Suppose  $u_0 \in L^2(\Omega)$ . Then for any given mesh size  $0 < h < L$ ,  $\langle \varepsilon(u^h) \rangle$  satisfies,

$$\langle \varepsilon(u^h) \rangle \leq C \left[ \frac{1}{\mathcal{R}e} \frac{L}{h} + \left( \frac{C_s \delta}{h} \right)^2 + \frac{L^5}{(C_s \delta)^4 h} + \frac{L^{\frac{5}{2}}}{(C_s \delta)^4} h^{\frac{3}{2}} \right] \frac{U^3}{L}.$$

*Proof.* The proof is very similar to the one of Theorem 3.1 except the estimation on the nonlinear term. Let fix  $h \in (0, L)$  from beginning. The strategy is to subtract off the inhomogeneous boundary conditions (1.2). The proof arises as well by taking  $v^h = u^h - \Phi$  in the finite element problem (2.8). Then after integrating with respect to time, we get (3.1). The proof continues by estimating each term on the right-hand side of (3.1). Using Lemma 2.1 and the Cauchy-Schwarz Young inequality, the first three terms on the RHS of the energy equality (3.1) can be estimated as,

$$(3.13) \quad (u^h(T), \Phi) \leq \frac{1}{2} \|u^h(T)\|^2 + \frac{1}{2} \|\Phi\|^2 = \frac{1}{2} \|u^h(T)\|^2 + \frac{1}{6} L^2 U^2 h.$$

$$(3.14) \quad (u^h(0), \Phi) \leq \|u^h(0)\| \|\Phi\| = \sqrt{\frac{h}{3}} U L \|u^h(0)\|.$$

$$(3.15) \quad \nu \int_0^T (\nabla u^h, \nabla \Phi) dt \leq \frac{\nu}{2} \int_0^T \|\nabla u^h\|^2 + \|\nabla \Phi\|^2 dt = \frac{\nu}{2} \int_0^T \|\nabla u^h\|^2 dt + \frac{\nu U^2 L^2}{2h} T.$$

Next applying the Young inequality,

$$ab \leq \frac{1}{p} a^p + \frac{1}{q} b^q,$$

for conjugate  $p = \frac{3}{2}$  and  $q = 3$  on  $a = |\nabla u^h|^2$  and  $b = |\nabla \Phi|$  gives,

$$(3.16) \quad \left| \int_{\Omega} |\nabla u^h| |\nabla u^h| |\nabla \Phi| dx \right| \leq \int_{\Omega} |\nabla u^h|^2 |\nabla \Phi| dx \leq \int_{\Omega} \left( \frac{2}{3} |\nabla u^h|^3 + \frac{1}{3} |\nabla \Phi|^3 \right) dx \leq \frac{2}{3} \int_{\Omega} |\nabla u^h|^3 dx + \frac{1}{3} \frac{U^3 L^2}{h^2}.$$

Inserting (3.13), (3.14), (3.15) and (3.16) in (3.1) implies,

$$(3.17) \quad \begin{aligned} & \frac{1}{2} \|u^h(T)\|^2 - \frac{1}{2} \|u^h(0)\|^2 + \nu \int_0^T \|\nabla u^h\|^2 dt + (C_s \delta)^2 \int_0^T \left( \int_{\Omega} |\nabla u^h|^3 dx \right) dt \leq \frac{1}{2} \|u^h(T)\|^2 + \frac{1}{6} L^2 U^2 h \\ & + \sqrt{\frac{h}{3}} U L \|u^h(0)\| + \frac{\nu}{2} \int_0^T \|\nabla u^h\|^2 dt + \frac{\nu U^2 L^2}{2h} T + \int_0^T b(u^h, u^h, \Phi) dt \\ & + \frac{2}{3} (C_s \delta)^2 \int_0^T \left( \int_{\Omega} |\nabla u^h|^3 dx \right) dt + \frac{1}{3} (C_s \delta)^2 \frac{U^3 L^2}{h^2} T. \end{aligned}$$

Finally the nonlinear term  $b(u^h, u^h, \Phi)$  is estimated as follow. First from Definition (2.2), we have,

$$(3.18) \quad |b(u^h, u^h, \Phi)| \leq \frac{1}{2} |(u^h \cdot \nabla u^h, \Phi)| + \frac{1}{2} |(u^h \cdot \nabla \Phi, u^h)|.$$

The first term on (3.18) can be estimated using the Hölder's inequality<sup>1</sup> for  $p = 3, q = 6$  and  $r = 2$ ,

$$|(u^h \cdot \nabla u^h, \Phi)| \leq \int_{\Omega} |u^h \nabla u^h \Phi| dx \leq \|\nabla u^h\|_3 \|u^h\|_6 \|\Phi\|_2,$$

<sup>1</sup>  $\int_{\Omega} |f g h| dx \leq \|f\|_p \|g\|_q \|h\|_r$  for  $\frac{1}{p} + \frac{1}{q} + \frac{1}{r} = 1$ .

then applying the following Young inequality <sup>2</sup> for conjugate exponents  $p = 3$  and  $q = \frac{3}{2}$ ,

$$(3.19) \quad ab \leq \frac{\epsilon}{3} a^3 + \frac{\epsilon^{-\frac{1}{2}}}{\frac{3}{2}} b^{\frac{3}{2}},$$

when  $a = \|\nabla u^h\|_3$ ,  $b = \|u^h\|_6 \|\Phi\|_2$  and  $\epsilon = \frac{(C_s \delta)^2}{4}$  leads to,

$$|b(u^h, u^h, \Phi)| \leq \frac{1}{12} (C_s \delta)^2 \|\nabla u^h\|_3^3 + \frac{2}{3} \left( \frac{(C_s \delta)^2}{4} \right)^{-\frac{1}{2}} \|\Phi\|_2^{\frac{3}{2}} \|u^h\|_6^{\frac{3}{2}}.$$

From Lemma 2.3 we have  $\|u^h\|_6 \leq C L^{\frac{1}{2}} \|\nabla u^h\|_3$ , it follows that

$$|b(u^h, u^h, \Phi)| \leq \frac{1}{12} (C_s \delta)^2 \|\nabla u^h\|_3^3 + \frac{2}{3} \left( \frac{(C_s \delta)^2}{4} \right)^{-\frac{1}{2}} \|\Phi\|_2^{\frac{3}{2}} C L^{\frac{3}{4}} \|\nabla u^h\|_3^{\frac{3}{2}}.$$

Again apply the general Young inequality for conjugate exponents  $p = 2$  and  $q = 2$  to the second term of the above inequality when  $\epsilon = \frac{(C_s \delta)^2}{6}$ ,

$$|(u^h \cdot \nabla u^h, \Phi)| \leq \frac{1}{6} (C_s \delta)^2 \|\nabla u^h\|_3^3 + \frac{1}{12} (C_s \delta)^2 \|\nabla u^h\|_3^3 + C \frac{8}{3} L^{\frac{3}{2}} (C_s \delta)^{-4} \|\Phi\|_2^3.$$

Use  $\|\Phi\|_2^3 = (\frac{h}{3})^{\frac{3}{2}} L^3 U^3$  from the Lemma 2.1 on the above inequality and then,

$$(3.20) \quad |(u^h \cdot \nabla u^h, \Phi)| \leq \frac{1}{6} (C_s \delta)^2 \|\nabla u^h\|_3^3 + C L^{\frac{3}{2}} (C_s \delta)^{-4} h^{\frac{3}{2}} L^3 U^3.$$

The second term  $|(u^h \cdot \nabla \Phi, u^h)|$  on (3.18) can be bounded first using the Hölder's inequality for  $p = 6, q = \frac{3}{2}$  and  $r = 6$ ,

$$|(u^h \cdot \nabla \Phi, u^h)| \leq \int_{\Omega} |u^h \nabla \Phi u^h| dx \leq \|\nabla \Phi\|_{\frac{3}{2}} \|\nabla u^h\|_3^2,$$

but  $\|u^h\|_6 \leq L^{\frac{1}{2}} \|\nabla u^h\|_3$ , Lemma 2.3, then,

$$|(u^h \cdot \nabla \Phi, u^h)| \leq \int_{\Omega} |u^h \nabla \Phi u^h| dx \leq \|\nabla \Phi\|_{\frac{3}{2}} L \|\nabla u^h\|_3^2,$$

then use the Young inequality (3.19) when  $a = \|\nabla u^h\|_3^2$  and  $b = \|\nabla \Phi\|_{\frac{3}{2}} L$  for  $p = \frac{3}{2}, q = 3$  and  $\epsilon = \frac{3}{16} (C_s \delta)^2$ ,

$$|(u^h \cdot \nabla \Phi, u^h)| \leq \frac{(C_s \delta)^2}{8} \|\nabla u^h\|_3^3 + \frac{16}{27} \frac{1}{(C_s \delta)^4} \|\nabla \Phi\|_{\frac{3}{2}}^3 L^3,$$

since  $\|\nabla \Phi\|_{\frac{3}{2}}^3 = \frac{U^3 L^4}{h}$ , Lemma 2.1, the above inequality turn to be,

$$(3.21) \quad |(u^h \cdot \nabla \Phi, u^h)| \leq \frac{(C_s \delta)^2}{8} \|\nabla u^h\|_3^3 + \frac{16}{27} \frac{U^3 L^7}{(C_s \delta)^4 h},$$

combining (3.20) and (3.21) in (3.18), we have the following estimate on the non-linearity,

$$(3.22) \quad |b(u^h, u^h, \Phi)| \leq \frac{7}{24} (C_s \delta)^2 \|\nabla u^h\|_3^3 + \frac{U^3 L^7}{(C_s \delta)^4 h} + \frac{L^{\frac{3}{2}} h^{\frac{3}{2}} L^3 U^3}{(C_s \delta)^4}.$$

Inserting (3.22) in (3.17) yields to,

---

<sup>2</sup>More generally, for conjugate  $(\frac{1}{p} + \frac{1}{q} = 1)$  exponents  $a \geq 0, b \geq 0 : ab \leq \frac{\epsilon}{p} a^p + \frac{\epsilon^{-\frac{q}{p}}}{q} b^q$  for any  $\epsilon \geq 0$ .

$$(3.23) \quad \begin{aligned} \frac{1}{2} \int_0^T \nu \|\nabla u^h\|^2 dt + \frac{1}{2} \int_0^T \left( \int_{\Omega} (C_s \delta)^2 |\nabla u^h|^3 dx \right) dt &\leq \frac{1}{2} \|u^h(0)\|^2 + \frac{1}{6} L^2 U^2 h \\ &+ \sqrt{\frac{h}{3}} U L \|u^h(0)\| + \frac{\nu U^2 L^2}{2h} T + \frac{1}{3} (C_s \delta)^2 \frac{U^3 L^2}{h^2} T + \frac{U^3 L^7}{(C_s \delta)^4 h} T + \frac{L^{\frac{3}{2}} h^{\frac{3}{2}} L^3 U^3}{(C_s \delta)^4} T. \end{aligned}$$

Note that the above inequality can justify the fact that the computed time-averaged of the energy dissipation of the solution (1.1) is uniformly bounded and hence  $\langle \varepsilon(u^h) \rangle$  is well-defined.

Dividing both side of the inequality (3.23) by  $|\Omega| = L^3$  and  $T$ , taking lim Sup as  $T \rightarrow \infty$  lead to,

$$\frac{1}{2} \langle \varepsilon(u^h) \rangle \leq \frac{1}{2} \frac{\nu U^2}{h L} + \frac{1}{3} (C_s \delta)^2 \frac{U^3}{h^2 L} + \frac{L^4 U^3}{(C_s \delta)^4 h} + \frac{h^{\frac{3}{2}} L^{\frac{3}{2}} U^3}{(C_s \delta)^4}.$$

Which can be written as

$$(3.24) \quad \langle \varepsilon(u^h) \rangle \leq C \left[ \frac{1}{\mathcal{R}e} \frac{L}{h} + \left( \frac{C_s \delta}{h} \right)^2 + \frac{L^5}{(C_s \delta)^4 h} + \frac{L^{\frac{5}{2}}}{(C_s \delta)^4} h^{\frac{3}{2}} \right] \frac{U^3}{L},$$

and the theorem is proved.  $\square$

*Remark 3.4.* The estimate in Theorem 3.3 is for a coarse mesh  $h \geq \mathcal{O}(\mathcal{R}e^{-1}) L$ . For the fully-resolved case  $h \rightarrow \mathcal{R}e^{-1}$  (or equivalently  $C_s \delta \rightarrow 0$ ), the other estimate in Theorem 3.1 takes over. More over, the estimate is independent of the viscosity at high Reynolds number. It is also dimensionally consistent.

The value of  $\langle \varepsilon(u^h) \rangle$  in Theorem 3.3 depends on three discretization parameters; the turbulence resolution length scale  $\delta$ , the Smagorinsky constant  $C_s$  and the numerical resolution  $h$ . These affect  $\langle \varepsilon(u^h) \rangle$ , but have no impact on the underlying velocity field  $u(x, t)$ , and hence they have no effect upon  $\langle \varepsilon(u) \rangle$ .

Consider the upper bound on  $\frac{\langle \varepsilon(u^h) \rangle}{U^3/L}$  in (3.24) as function of  $(C_s \delta)$  and  $h$ , when  $\mathcal{R}e \gg 1$  and  $L$  are being fixed. The expression includes three main terms. The terms in the estimate are associated with physical effects as follows,

- (1)  $\lambda_1(h, C_s \delta) = \frac{1}{\mathcal{R}e} \frac{L}{h} \implies$  Viscosity,
- (2)  $\lambda_2(h, C_s \delta) = \left( \frac{C_s \delta}{h} \right)^2 \implies$  Model Viscosity,
- (3)  $\lambda_3(h, C_s \delta) = \frac{L^5}{(C_s \delta)^4 h} + \frac{L^{\frac{5}{2}}}{(C_s \delta)^4} h^{\frac{3}{2}} \implies$  Non-linearity.

Tracking back the proof of Theorem 3.3,  $\lambda_1$ ,  $\lambda_2$  and  $\lambda_3$  correspond to the viscosity term  $\nu \Delta u$ , model viscosity  $\nabla \cdot ((C_s \delta)^2 |\nabla u| \nabla u)$  and non-linear term  $u \cdot \nabla u$  respectively. The three level sets of  $\lambda_1 = \lambda_2$ ,  $\lambda_2 = \lambda_3$  and  $\lambda_1 = \lambda_3$  are respectively denoted by the curves  $\zeta_1$ ,  $\zeta_2$  and  $\zeta_3$  in the Figure 3, which are calculated as,

- (1)  $\zeta_1 : \lambda_1 = \lambda_2 \implies C_s \delta = \mathcal{R}e^{-\frac{1}{2}} L \left( \frac{h}{L} \right)^{\frac{1}{2}},$
- (2)  $\zeta_2 : \lambda_2 = \lambda_3 \implies C_s \delta = L \left[ \left( \frac{h}{L} \right)^{\frac{7}{2}} + \frac{h}{L} \right]^{\frac{1}{6}},$
- (3)  $\zeta_3 : \lambda_1 = \lambda_3 \implies C_s \delta = \mathcal{R}e^{\frac{1}{4}} L \left[ 1 + \left( \frac{h}{L} \right)^{\frac{5}{2}} \right]^{\frac{1}{4}}.$

*Remark 3.5.* Consider the horizontal axis to be  $\frac{h}{L}$  and the vertical one to be  $C_s \delta$ . The three level sets divide the  $(\frac{h}{L})(C_s \delta)$  - plane to the four regions. The four regions I, II, III and IV are identified with respect to the comparative magnitude size of  $\lambda_1$ ,  $\lambda_2$  and  $\lambda_3$  on the  $(\frac{h}{L})(C_s \delta)$  - plane, Figure 3. After comparing the magnitude of these three functions on each separate region, it can be seen that below the curve  $\zeta_2$  (regions I and II) the effect of non-linearity term  $u \cdot \nabla u$  on energy dissipation, corresponding to  $\lambda_3$ , dominates the other other terms. But above the curve  $\zeta_2$  (regions III and IV) the model viscosity term, corresponding to

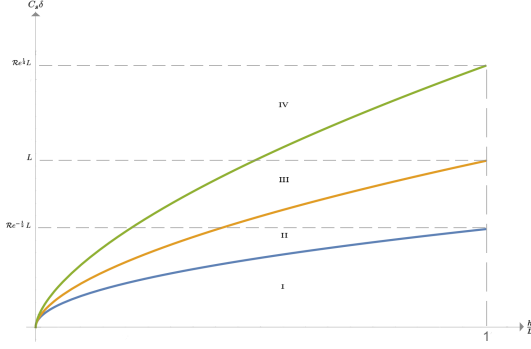


FIGURE 3. Level Sets

$\lambda_2$ , dominates. Surprisingly, the viscosity term  $\nu \Delta u$  is never bigger than the other two terms for any choice of  $h$ ,  $\delta$  and  $C_s$ .

The Smagorinsky coefficient  $C_s$  can be calibrated for a given class of flows. Its values varies from flow to flow and from domain to domain (see e.g. Page 23 of Galperin and Orszag [13] who quote a range  $0.000744 \leq C_s \leq 0.020$ ). In the next corollary the optimal value, with respect to the current analysis, of  $C_s$  in the Theorem 3.3 is investigated, considering  $\delta = h$  which is a common choice [36].

**Corollary 3.6.** *Let  $\delta = h \geq \mathcal{O}(\text{Re}^{-1})L$  be fixed. Then for any choice of  $C_s > 0$ , the upper estimate on  $\frac{\langle \varepsilon(u^h) \rangle}{U^3/L}$  in the Theorem 3.3 is larger than dissipation coefficient  $C_\epsilon$  in Figure 2.*

*Proof.* Letting  $\delta = h$ , Theorem 3.3 suggests,

$$(3.25) \quad \frac{\langle \varepsilon(u^h) \rangle}{U^3/L} \simeq \frac{1}{\text{Re}} \frac{L}{h} + C_s^2 + \frac{1}{C_s^4} \left[ \left( \frac{L}{h} \right)^5 + \left( \frac{L}{h} \right)^{\frac{5}{2}} \right].$$

Solving the minimization problem  $(C_s)_{\min} = \arg \min_{C_s} F(C_s)$ , the minimum of the function,

$$(3.26) \quad F(C_s) = \frac{1}{\text{Re}} \frac{L}{h} + C_s^2 + \frac{1}{C_s^4} \left[ \left( \frac{L}{h} \right)^5 + \left( \frac{L}{h} \right)^{\frac{5}{2}} \right],$$

occurs at

$$(3.27) \quad F_{\min} = \frac{1}{\text{Re}} \frac{L}{h} + 2 \left[ \left( \frac{L}{h} \right)^5 + \left( \frac{L}{h} \right)^{\frac{5}{2}} \right]^{\frac{1}{3}},$$

for  $(C_s)_{\min} = \sqrt[6]{2} \left[ \left( \frac{L}{h} \right)^5 + \left( \frac{L}{h} \right)^{\frac{5}{2}} \right]^{\frac{1}{6}}$ , assuming  $\mathcal{O}(\text{Re}^{-1}) < \frac{h}{L} < 1$  is fixed. This minimum amount (3.27) dramatically exceed the range of  $C_\epsilon$  in Figure 2 for any typical choice of  $h$  in LES.  $\square$

*Remark 3.7.* Corollary 3.6 indicates over-dissipation of  $\langle \varepsilon(u^h) \rangle$  for any choose of  $C_s > 0$ . As an example, let  $\frac{h}{L} = 0.01$ , then  $F_{\min} \simeq 2000$  in (3.27) as  $\text{Re} \rightarrow \infty$ . It is much larger than the experimental range of  $C_s$  in Figure 2,  $\frac{1}{\text{Re}} \leq C_s \leq 0.1$ , see Figure 4.

However  $\delta = \mathcal{O}(h)$  in many literature [36], the relationship between the grid size  $h$  and the filter size  $\delta$  have been made based on heuristic instead of a sound numerical analysis (p.26 of [4]). Therefore for an LES of fixed computational cost (i.e. fixed  $h$ ) and fixed length scale  $L$ , one can ask how artificial parameter  $C_s \delta$  should be selected such that the statistics of the model be consistent with numerical and experimental evidence

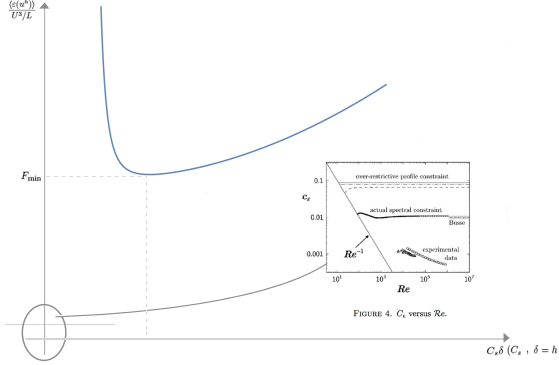


FIGURE 4. Theorem 3.3 vs experimental results in Figure 2.

summarized in Figure 2. To answer this question, the inequality (3.24) takes over in the next corollary for under-resolved spacial mesh  $h \geq \mathcal{O}(\mathcal{R}e^{-1})L$ , since no model is used when (at much greater cost) a DNS is performed with  $\frac{h}{L} \simeq \mathcal{R}e^{-1}$ .

**Corollary 3.8.** *Let the mesh size  $h \geq \mathcal{O}(\mathcal{R}e^{-1})L$  be fixed. Then for any choice of  $C_s > 0$  and  $\delta > 0$ , the upper estimate on  $\frac{\langle \varepsilon(u^h) \rangle}{U^3 / L}$  in the Theorem 3.3 is larger than dissipation coefficient  $C_\epsilon$  in Figure 2.*

*Proof.* Solving the minimization problem  $(C_s \delta)_{\min} = \arg \min_{C_s \delta} G(C_s \delta)$ , the minimum of the function,

$$(3.28) \quad G(C_s \delta) = \frac{1}{\mathcal{R}e} \frac{L}{h} + \left( \frac{C_s \delta}{h} \right)^2 + \frac{L^5}{(C_s \delta)^4 h} + \frac{L^{\frac{5}{2}}}{(C_s \delta)^4} h^{\frac{3}{2}},$$

occurs at,

$$F_{\min} = \frac{1}{\mathcal{R}e} \frac{L}{h} + 2 \left[ \left( \frac{L}{h} \right)^5 + \left( \frac{L}{h} \right)^{\frac{5}{2}} \right]^{\frac{1}{3}},$$

for  $(C_s \delta)_{\min} = \sqrt[6]{2} h \left[ \left( \frac{L}{h} \right)^5 + \left( \frac{L}{h} \right)^{\frac{5}{2}} \right]^{\frac{1}{6}}$  assuming  $h$  and  $L$  are fixed. This minimum amount which is much larger than the experimental range of  $C_\epsilon$ ,  $\frac{1}{\mathcal{R}e} \leq C_\epsilon \leq 0.1$ , leads over-dissipation of the model, Figure 4.  $\square$

**Remark 3.9.** The extra dissipation in the Corollary 3.6 and 3.8, which is consistent with experience with the Smagorinsky model (e.g., Iliescu and Fischer [19] and Moin and Kim [31]), can laminarize the numerical approximation of a turbulent flow and prevent the transition to turbulence.

**Remark 3.10.** In the limit of high Reynolds number and for a fix computational cost  $h \geq \mathcal{O}(\mathcal{R}e^{-1})L$ , the estimate in Theorem 3.3 is the function of  $C_s \delta$ ,

$$\frac{\langle \varepsilon(u^h) \rangle}{U^3 / L} \simeq \left( \frac{C_s \delta}{h} \right)^2 + \frac{1}{(C_s \delta)^4} \left[ \frac{L^5}{h} + L^{\frac{5}{2}} h^{\frac{3}{2}} \right],$$

which consists of two major parts. First,

$$\lambda_2 = \mathcal{O}((C_s \delta)^2)$$

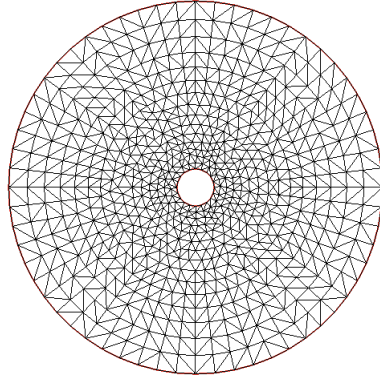


FIGURE 5. Coarse mesh with 60 mesh points on the outer and 20 points on the inner circle.

is derived from the eddy viscosity term and is quadratic in  $(C_s\delta)$ . The latter,

$$\lambda_3 = \mathcal{O}((C_s\delta)^{-4})$$

is derived from the non-linearity term and is inversely proportional to  $(C_s\delta)^4$ . Therefore, the behavior of the graph  $\frac{\langle \varepsilon(u^h) \rangle}{U^3/L}$  in Figure 4 is decided by the competition between the increasing function  $\lambda_2$  and the decreasing function  $\lambda_3$ . This observation suggests model over-dissipation is due to the action of the model viscosity, which is also consistent with [23]. Analysis in [23] suggested that the model over-dissipation is due to the action of the model viscosity in boundary layers rather than in interior small scales generated by the turbulent cascade.

#### 4. NUMERICAL SIMULATIONS

The test is a comparison between simulation of the NSE and the Smagorinsky model for two dimensional time-dependent shear flow between two cylinders, motivated by the classic problem of flow between rotating cylinders. The domain is a disk with a smaller center obstacle inside. The flow is driven by the rotational force at the outer circle in an absence of body force, with no-slip boundary conditions suppressed on the inner circle. Note that in an absent of body force here, most of the interesting structures are expected to be due to the interaction of the flow with the boundaries. The tests were performed using FreeFEM++ [16], with Taylor-Hood elements (continuous piecewise quadratic polynomials for the velocity and continuous linear polynomials for the pressure) in all tests. The under-resolved mesh is parameterized by the number of mesh points  $m = 60$  around the outer circle and  $n = 20$  mesh points around the immersed circle and extended to all of the domain as a Delaunay mesh, Figure 5. We take  $\mathcal{R}e = 3000$ , final time  $T = 10$  and time step  $\Delta t = 0.01$ . The initial condition  $u_0$  is generated by solving the steady Stokes problem with the same condition describe above on the same geometry, this gives initial condition that is divergence free and satisfy the boundary conditions. The Backward Euler method is utilized for time discretization.

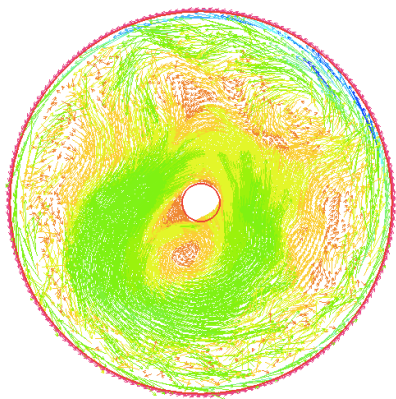
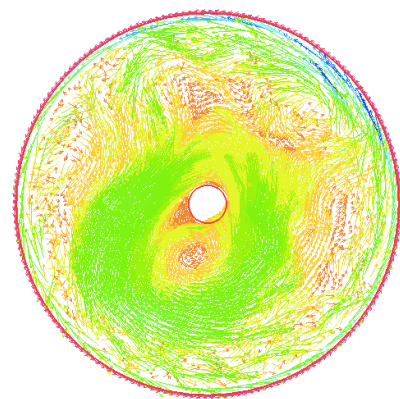


FIGURE 6. NSE.

FIGURE 7. SM as  $C_s \rightarrow 0$ .

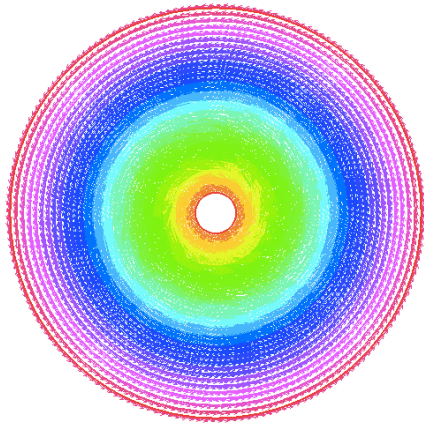
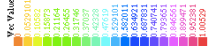
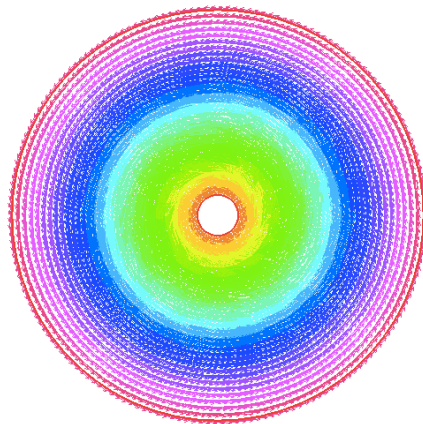
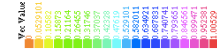
In the NSE (Figure 6), as it is expected, flow does not approach a steady state and the chaotic behavior of the velocity field specially near the boundaries can be seen. To verify the code works properly,  $C_s = 0.00001$  (i.e.  $C_s \rightarrow 0$ ) is considered once in the SM. The same chaotic behavior as the NSE is observed in this scenario and the result is quite identical, which is consistent with the fact that  $SM \rightarrow NSE$  as  $C_s \rightarrow 0$  (Figure 7).

To run the test on the Smagorinsky model, providing all other conditions hold, consider  $C_s = 0.17$  [26]. Motivated from Corollaries 3.6 and 3.8 consider  $\delta = h$  (Figure 8) and  $\delta = h^{\frac{1}{6}}$  (Figure 9). In all cases, the model predicts the flow will quickly reach a nonphysical equilibrium, which is clearly over-dissipated. This extra dissipation laminarizes the approximation of the flow and prevent the transition to turbulence.

## 5. CONCLUSION

We investigate the computed time-averaged energy dissipation  $\langle \varepsilon(u^h) \rangle$  here for shear flow turbulence on the under-resolved mesh.  $\langle \varepsilon(u^h) \rangle$  scales as the equilibrium dissipation law,  $\frac{U^3}{L}$ , for under-resolved mesh independent of  $\nu$  at high Reynolds number being considered. The upper bound in Theorem 3.3 does not give the correct dissipation for any choice of the Smagorinsky constant  $C_s > 0$  and filter size  $\delta > 0$ , which is consistent with the numerical evidence. In addition, it is shown that the viscosity term  $\nu \Delta u$  does not affect  $\langle \varepsilon(u^h) \rangle$  for any choice of discretization parameters. The next important step would be analyzing the computed energy dissipation rate for other turbulent models, e.g. dynamic subgrid-scale model, on an under-resolved spacial mesh.

The analysis here indicates that the model over-dissipation is due to the action of the eddy viscosity term  $\nabla \cdot ((C_s \delta) |\nabla u| \nabla u)$ . The classical approach to correct the over-dissipation of the Smagorinsky model is to multiply the eddy viscosity term with damping function. The mathematical analysis in [35] shows that the combination of the Smagorinsky with a modified van Driest damping does not over dissipate assuming infinite

FIGURE 8. SM,  $\delta = h$ .FIGURE 9. SM,  $\delta = h^{\frac{1}{6}}$ .

resolution (i.e. continuous case). The unexplored question is: What is the statistics of this combination on an under-resolved mesh size?

In this report, the Smagorinsky model is used instead of the NSE. One can try to calculate the energy dissipation rate for the discretized NSE on the coarse mesh. The key part of the success is to prove the boundedness of the kinetic energy of the approximate velocity,  $\|u^h\|^2$ , for the NSE without any restriction on the mesh size  $h$ .

**Acknowledgments.** The author is extremely grateful to Professor William Layton from whom he has learned so much about fluid dynamics and mathematics. A.P. was Partially supported by NSF grants, DMS 1522267 and CBET 1609120.

## REFERENCES

- [1] R. A. Antonia and B. R. Pearson, *Effect of initial conditions on the mean energy dissipation rate and the scaling exponent*, Physical Review E **62** (2000), 8086-8090.
- [2] R. A. Antonia, B. R. Satyaprakash, and A. K. M. F. Hussain, *Measurements of dissipation rate and some other characteristics of turbulent plane and circular jets*, Physics of Fluids **23** (1980), 695-700.
- [3] G. K. Batchelor, *The theory of homogeneous turbulence*, Cambridge University Press, Cambridge, England, 1953.
- [4] L.C. Berselli, T. Iliescu, and W.J. Layton, *Mathematics of large eddy simulation of turbulent flows*, Scientific Computation, Springer-Verlag, Berlin, 2006.
- [5] W. Bos, L. Shao, and J. P. Bertoglio, *Spectral imbalance and the normalized dissipation rate of turbulence*, Physics of Fluids **19** (2007).
- [6] P. Burattini, P. Lavoie, and R. A. Antonia, *On the normalized turbulent energy dissipation rate*, Physics of Fluids **17** (2005).
- [7] F.H. Busse, *Bounds for turbulent shear flow*, Journal of Fluid Mechanics **41** (1970), 4219-240.

- [8] J. Davila and J. C. Vassilicos, *Richardsons Pair Diffusion and the Stagnation Point Structure of Turbulence*, Physical review letters **91** (2003).
- [9] C.R. Doering and P. Constantin, *Energy dissipation in shear driven turbulence*, Physical review letters **69** (1992), 1648.
- [10] Q. Du and M. D. Gunzburger, *Finite-element approximations of a Ladyzhenskaya model for stationary incompressible viscous flow*, SIAM J. Numer. Anal. **27** (1990), no. 1, 1–19.
- [11] U. Frisch, *Turbulence: The Legacy of A. N. Kolmogorov*, Cambridge University Press, 1995.
- [12] M. Gad-el-Hak and S. Corrsin, *Measurements of the nearly isotropic turbulence behind a uniform jet grid*, Journal of Fluid Mechanics **62** (1974), 115–143.
- [13] B. Galperin and S. A. Orszag, *Large eddy simulation of complex engineering and geophysical flows*, Cambridge University Press, 1993.
- [14] V. Girault and P.A. Raviart, *Finite element approximation of the Navier-Stokes equations*, Lecture Notes in Mathematics, vol. 749, Springer-Verlag, Berlin-New York, 1979.
- [15] S. Goto and J. C. Vassilicos, *The dissipation rate coefficient of turbulence is not universal and depends on the internal stagnation point structure*, Physics of Fluids **21** (2009).
- [16] F. Hecht, *New development in FreeFEM++*, J. Numer. Math. **20** (2012), 251265.
- [17] E. Hopf, *Lecture series of the symposium on partial differential equations*, Berkeley, 1955.
- [18] L.N. Howard, *Bounds on flow quantities*, Annual Review of Fluid Mechanics **4** (1972), 473–494.
- [19] T. Iliescu and P. Fischer, *Backscatter in the rational LES model*, Computers and Fluids **33** (2004), 783–790.
- [20] V. John, W.J. Layton, and C. C. Manica, *Convergence of Time-Averaged Statistics of Finite Element Approximations of the NavierStokes Equations*, SIAM J. Numer. Anal. **46**(1) (2007), 151–179.
- [21] R.R. Kerswell, *Variational bounds on shear-driven turbulence and turbulent Boussinesq convection*, Physica D **100** (1997), 355–376.
- [22] D.P. Lathrop, J. Fineberg, and H. L. Swinney, *Turbulent flow between concentric rotating cylinders at large Reynolds number*, Physical review letters **68** (1992), no. 10, 1515.
- [23] W.J. Layton, *Energy dissipation in the Smagorinsky model of turbulence*, Appl. Math. Lett. **59** (2016), 56–59.
- [24] W.J. Layton, *Energy dissipation bounds for shear flows for a model in large eddy simulation*, Math. Comput. Modelling **35** (2002), no. 13, 1445–1451.
- [25] W.J. Layton, *Introduction to the numerical analysis of incompressible viscous flows*, Computational Science & Engineering, vol. 6, Society for Industrial and Applied Mathematics (SIAM), Philadelphia, PA, 2008. With a foreword by Max Gunzburger.
- [26] D.K. Lilly, *The representation of small-scale turbulence in numerical simulation experiments*, IBM Scientific Computing Symposium on Environmental Sciences (1967).
- [27] J. L. Lumley, *Some comments on turbulence*, Physics of Fluids A **4** (1992), 203–211.
- [28] C. Marchioro, *Remark on the energy dissipation in shear driven turbulence*, Phys. D **74** (1994), no. 3-4, 395–398.
- [29] N. Mazellier and C. Vassilicos, *The turbulence dissipation constant is not universal because of its universal dependence on large-scale flow topology*, Physics of Fluids **20** (2008).
- [30] W. D. McComb, A. Berera, S. R. Yoffe, and M. F. Linkmann, *Energy transfer and dissipation in forced isotropic turbulence*, Phys. Rev. E **91** (2015).
- [31] P. Moin and J. Kim, *Numerical investigation of turbulent channel flow*, Journal of Fluid Mechanics **118** (1982), 341–377.
- [32] R. Moser, J. Kim, and N. Mansour, *Direct Numerical Simulation of Turbulent Channel Flow up to  $Re_\tau=590$* , Phys. Fluids **11** (1998), 943945.
- [33] R. Nicodemus, S. Grossmann, and M. Holthaus, *Towards lowering dissipation bounds for turbulent flows*, The European Physical Journal B **10** (1999), no. 2, 385–396.
- [34] R. Nicodemus, S. Grossmann, and M. Holthaus, *Variational bound on energy dissipation in plane Couette flow*, Physical Review E **56** (1997), no. 6, 6774.
- [35] A. Pakzad, *Damping functions correct over-dissipation of the Smagorinsky Model*, Mathematical Methods in the Applied Sciences **40** (2017), no. 16, 5933–5945, DOI 10.1002/mma.4444.
- [36] S. B. Pope, *Ten questions concerning the large-eddy simulation of turbulent flows*, New Journal of Physics **6** (2004).
- [37] H. Reichardt, *Gesetzmäßigkeiten der geradlinigen turbulenten Couettestromung*, Report No. 22 of the Max-Planck-Institut für Stromungsforschung und Aerodynamische versuchsanstalt, Gottingen (1959).
- [38] L. F. Richardson, *weather prediction by numerical process*, Cambridge, UK: Cambridge Univ. Press, 1922.
- [39] P.G. Saffman, *485-614 in: Topics in Nonlinear Physics, N. Zabusky (ed.)*, Springer-Verlag, New York, 1968.

- [40] P. Sagaut, *Large eddy simulation for incompressible flows*, Scientific Computation, Springer-Verlag, Berlin, 2001. An introduction; With an introduction by Marcel Lesieur; Translated from the 1998 French original by the author.
- [41] K. R. Sreenivasan, *The energy dissipation in turbulent shear flows*, Symposium on Developments in Fluid Dynamics and Aerospace Engineering, 1995, pp. 159–190.
- [42] K.R. Sreenivasan, *An update on the energy dissipation rate in isotropic turbulence*, Phys. Fluids **10** (1998), no. 2, 528–529.
- [43] G. I. Taylor, *statistical theory of turbulence*, Proc. R. Soc. Lond A 151:421-44 (1935).
- [44] D. J. Tritton, *Physical Fluid Dynamics*, 2nd edition, Oxford Science Publications, 1988.
- [45] X. Wang, *Approximation of stationary statistical properties of dissipative dynamical systems: time discretization*, Mathematics of Computation **79** (2010), no. 269, 259-280.
- [46] X. Wang, *Time-averaged energy dissipation rate for shear driven flows in  $\mathbf{R}^n$* , Phys. D **99** (1997), no. 4, 555–563.